

# Mixing Enhancement in a Micro Serpentine Conduit for Cell Sorting

Chainarong Chaktranond<sup>1</sup>, Koji Fukagata<sup>2</sup>, Nobuhide Kasagi<sup>3</sup>

1: Dept. of Mechanical Engineering, The University of Tokyo, Japan, chainaro@thtlab.t.u-tokyo.ac.jp

2: Dept. of Mechanical Engineering, The University of Tokyo, Japan, fukagata@thtlab.t.u-tokyo.ac.jp

3: Dept. of Mechanical Engineering, The University of Tokyo, Japan, kasagi@thtlab.t.u-tokyo.ac.jp

---

**Abstract** Lagrangian particle tracking simulations are performed on motions of cells and magnetic beads in a micro serpentine conduit designed as a mixer for a micro cell sorting system. Mixing of magnetic beads is enhanced, under the condition of low Reynolds number, by applying time-varying magnetic forces. Different conditions of magnetic forcing are examined and the efficiency of the mixer is measured by different indices. The mechanism to enhance the mixer efficiency is investigated in detail.

---

## 1. Introduction

Immuno-magnetic cell sorting is a reliable technique (Chalmers et al., 1998) to effectively separate target cells from cell-mixture in the following manner. First, magnetic beads coated with an antibody attach the target cells that have the corresponding antigen. After the attachment, only the cell attached by the beads can be isolated from the mixture by using magnetic forces.

Existing immuno-magnetic cell sorters are designed to process relatively large amount of cell mixture, say, on order of one liter. In contrast, R&D studies of micro-scale immuno-magnetic cell sorters are actively done as a part of micro-Total-Analysis-System, also known as, Lab-on-a-Chip. One of the key issues for successful development of such a micro immuno-magnetic cell sorter is effective mixing of beads and cells in a flow of buffer fluid at an extremely low-Reynolds number environment. For this issue, two strategies have been proposed. One is passive mixing, which uses conduits with complicated geometry (Branebjerg et al., 1996; Beebe et al., 2001). The other is active mixing, which uses external forcing, such as pressure perturbations (Vorperet et al., 2002; Niu and Lee, 2003), dielectrophoretic forces (Deval et al., 2002), or magnetic forced (Suzuki et al., 2004), all to realize so-called chaotic mixing (Ottino, 1989).

In the studies above, the efficiency of mixer is usually measured by the largest Lyapunov exponent. The use of this index is fair if only the motion of magnetic beads is of interest, as is in the cases of Deval et al. (2002) and Suzuki et al. (2004). However, when a mixture of beads and cells is of interest, as is in the cases of actual cell sorters, the largest Lyapunov exponent may fail to measure the performance of mixers.

The objective of the present study is, at first, to numerically investigate on the relation among different indices to measure the performance of active mixers. Here, we consider the magnetic mixer of Suzuki et al. (2004) and perform Lagrangian particle tracking simulations of the motion of magnetic beads and cells in this mixer. Subsequently, the mechanism to increase the performance is investigated under different forcing conditions.

## 2. Computational model

### 2.1 Micro serpentine conduit

We consider an immuno-magnetic micro-mixer proposed by Suzuki et al. (2004), as shown in Fig. 1. One unit of the conduit is 160  $\mu\text{m}$  long, 80  $\mu\text{m}$  wide and 35  $\mu\text{m}$  deep. In each mixer unit,

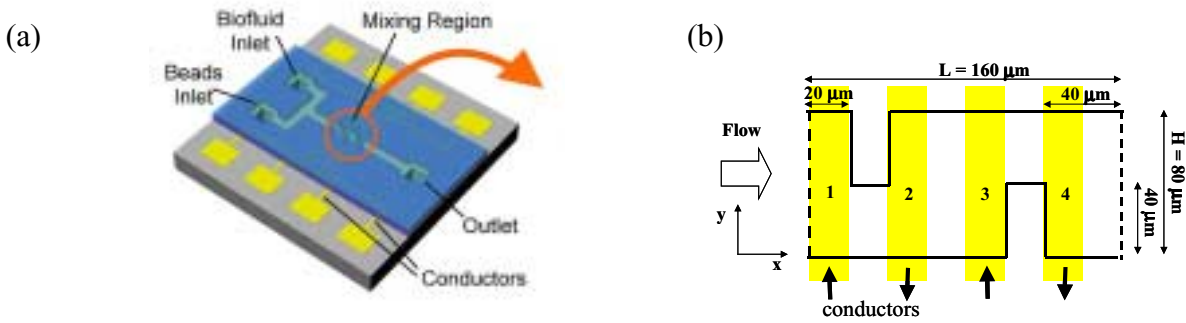


Fig. 1. Immuno-magnetic micro-mixer proposed by Suzuki et al. (2004).

(a) Overview of conduit; (b) Geometry and location of conductors in one unit.

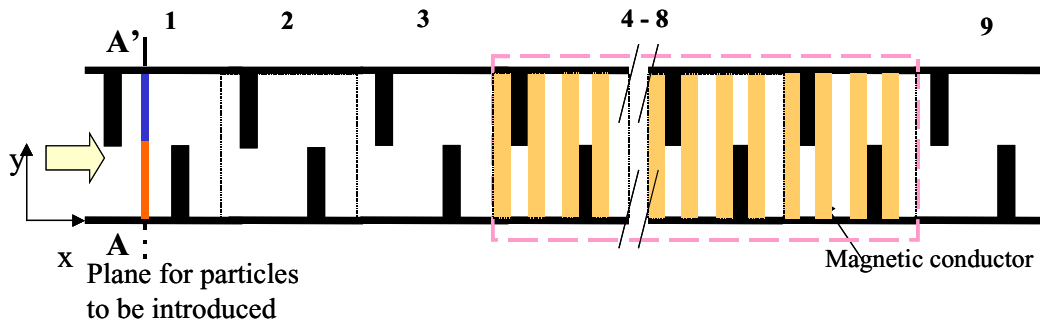


Fig. 2. Computational model.

four parallel magnetic conductors (labeled as 1 to 4) are embedded with equal spacing in the bottom wall. The conductors work to generate time-dependent magnetic force so that the immuno-magnetic beads move across the streamlines, as exemplified in Fig. 1b.

In the present simulations, we deal with a two-dimensional plane of that mixer, as shown in Fig. 2. We assume that the plane is located at  $5 \mu\text{m}$  above the bottom wall, at which effects of surface forces (e.g., Ho and Tai, 1998) can be neglected. The mixer has a finite length and consists of nine units (denoted as Unit 1 to Unit 9). The flow direction is from left to right. The immuno-magnetic beads (displayed in blue) and the cells (red) are introduced, respectively, in the upper and lower halves of section A-A' in Unit 1. Initial positions of beads/cells within the section A-A' are given by uniform random numbers. The main body of the mixer, where the magnetic force is applied, extends from Unit 4 to Unit 8.

## 2.2 Lagrangian particle tracking

Trajectories of the beads and cells are computed by using one-way coupling Lagrangian particle tracking simulations in the above-mentioned two-dimensional plane.

The fluid is assumed Newtonian and incompressible. The velocity field, which is stationary, is calculated by using the finite difference method on a regular grid system. The number of grids is 80 and 40 in the streamwise ( $x$ ) and wall-normal ( $y$ ) directions, respectively. The bulk Reynolds number is very low, i.e.,  $Re_b = U_b H/\nu = 0.0032$ , where  $U_b$  is the bulk mean velocity,  $H$  is width of the mixer, and  $\nu$  is the kinematic viscosity.

We assume for simplicity the beads and cells to be rigid spheres of  $1 \mu\text{m}$  in diameter, although in reality cells are deformable and their typical diameter is on order of  $10 \mu\text{m}$ . Brownian motion is neglected. Thus, the simplified particle equation of motion reads

$$\frac{d\vec{u}_p}{dt} = \frac{1}{\tau_p}(\vec{u}_f - \vec{u}_p) + \frac{\vec{F}}{m_p}, \quad (1)$$

where  $\vec{u}_p$  and  $\vec{u}_f$  are, the velocity of particle and fluid, respectively,  $\tau_p = \rho_p d_p^2 / (18\mu_f)$  is the particle relaxation time, and  $\vec{F}(\vec{x}, t)$  is the magnetic force. The quantities at the particle position,  $\vec{u}_f$  and  $\vec{F}$ , are interpolated from the grids by using the bilinear interpolation scheme. The time integration for the velocity and position of particles is done by using the Crank-Nicolson scheme.

Collisions among beads and among cells are neglected and only binary collisions between a bead and a cell are considered. When the distance between their center positions ( $\vec{x}_b$  and  $\vec{x}_c$ , respectively) becomes less than the summation of their radii ( $r_b$  and  $r_c$ ), i.e.,

$$|\vec{x}_b - \vec{x}_c| \leq r_b + r_c, \quad (2)$$

the bead is assumed to immediately attach the cell. Attachment of multiple beads to a single cell is allowed, similarly to actual situations. After a cell is attached by beads, the beads and the cell move together. To simplify the calculation of magnetic and drag forces, the cell combined with beads is treated as a single sphere with an equivalent diameter, mass and magnetic property.

### 2.3 Magnetic force

The magnetic forces are generated by the conductors embedded in the bottom wall of the mixer, as shown in Fig. 3. The conductors are assumed infinitely long. From the Biot-Savart law, the magnetic force,  $\vec{F}$ , on a magnetic bead can be expressed as

$$\vec{F} = \mu_r (1 - N_d) V_m (\vec{H} \cdot \nabla) \vec{B}, \quad (3)$$

where  $\vec{B} = \mu_0 \vec{H}$  is the magnetic flux density,  $\mu_0$  and  $\mu_r$  are the permeability in vacuum ( $\mu_0 = 4\pi \times 10^{-7}$  H/m) and the relative permeability, respectively,  $V_m$  is the volume of magnetic bead, and  $N_d$  is the demagnetizing factor ( $N_d = 0.333$  for a sphere). The relative permeability is a property of the magnetic bead. In this study, we assume calboxyl-polystyrene ( $\mu_r = 11.3$ ,  $\rho_p = 1500$  kg/m<sup>3</sup>) as the material of magnetic beads, similarly to the experiment by Suzuki et al. (2004). This material is paramagnetic. Namely, the beads have no magnetic memory after removing the magnetic force.

The electric current is imposed on the conductors in the sequence of (4 & 1) → (1 & 2) → (2 & 3) → (3 & 4), as shown in Fig. 3a, and these phases are referred to as Phase I to Phase IV. As an example, the distribution and directions of magnetic forces in Phase III are shown in Fig. 3b.

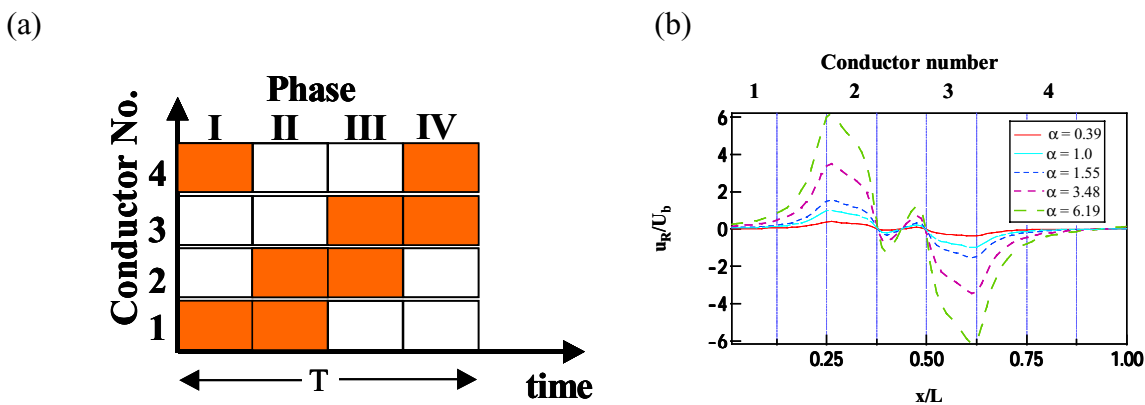


Fig. 3. Magnetic force.

(a) Operation diagram; (b) Distribution of non-dimensionalized magnetic force in Phase III.

### 3. Parameters and measures

#### 3.1 Parameters

##### Strouhal number

The Strouhal number,  $Str$ , is defined for the magnetic actuation. By using the frequency of the sequence of Phase I to Phase IV,  $f$ , and the distance between two conductors,  $L / 4$ , the Strouhal number is defined as

$$Str = \frac{fL / 4}{U_b} = \frac{L}{4U_b T}. \quad (4)$$

##### Amplitude factor

Because the particle relaxation time is extremely short, the magnetic force is nearly balanced by the drag force at any instants. Therefore, the maximum relative velocity between fluid and particle is  $u_{R,\max} \approx F_{\max} \tau_p / m_p$ , where  $F_{\max}$  is the maximum magnetic force. We define a non-dimensional amplitude of magnetic force,  $\alpha$ , (hereafter referred to as the amplitude factor) as the ratio of  $u_{R,\max}$  to  $U_b$ , i.e.,

$$\alpha = \frac{u_{R,\max}}{U_b} = \frac{F_{\max} \tau_p}{m_p U_b}. \quad (5)$$

#### 3.2 Measures of mixer performance

##### Lyapunov exponent

The largest Lyapunov exponent,  $\lambda$ , is defined as

$$\lambda = \lim_{t \rightarrow \infty} \left[ \frac{1}{t} \ln \left| \frac{dx(t)}{dx(0)} \right| \right], \quad (6)$$

where  $dx(0)$  and  $dx(t)$  are the distance between two nearby points at initial time and time  $t$ , respectively. This index indicates the average exponential rates of divergence or convergence of nearby points. In order to calculate this index, we use a method with reinitialization proposed by Sprott (2000) and used by Niu and Lee (2003) and Suzuki et al. (2004).

##### Contact number

We define a contact number,  $n_c$ , as the number of cells attached by beads. By using this, we also define a contact ratio,  $\gamma$ , as the percentage ratio of the number of cells attached by beads to the total number of cells exiting from the outlet,  $N_c$ , i.e.,

$$\gamma = \frac{n_c}{N_c} \Big|_{outlet} \times 100 [\%]. \quad (7)$$

For practical immuno-magnetic cell sorters, it is preferable to use less magnetic particles in order to reduce the running cost. Therefore, we introduce a cost function, i.e.,

$$J = \frac{\ell N_b}{n_c} \Big|_{outlet}, \quad (8)$$

where  $\ell$  is the price of a antibody-coated magnetic bead. This cost function indicates the price for the beads used to separate one target cell.

### 3. Results and Discussions

Efficiency of the mixer is evaluated under different conditions of magnetic force i.e.,  $\alpha = 0.39 - 6.19$  and  $Str = 0.25 - 2$ . The ratio of the number of beads to that of cells is unity. The area fraction of the particles (i.e., beads and cells) is about  $3.2 \times 10^{-3}$ . Without magnetic force, both the beads and cells follow the fluid streamlines, as shown in Fig. 4. As the result,  $\lambda$  is zero, as shown in Fig. 5.

With the magnetic force, the beads move across the fluid streamlines, as shown in Fig. 6, and the mixing is enhanced. Two indices ( $\lambda$  and  $\gamma$ ) exhibit different behaviors. Larger amplitude ( $\alpha$ )

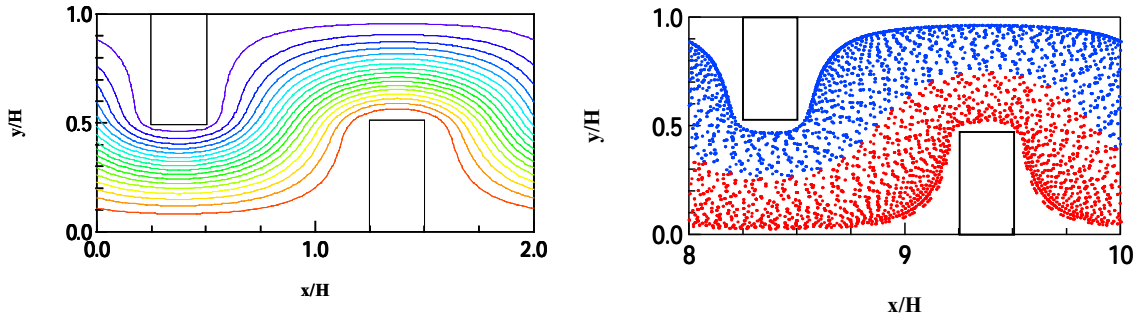


Fig. 4. Without magnetic force.

(a) Fluid streamlines; (b) Positions of beads (blue) and cells (red).

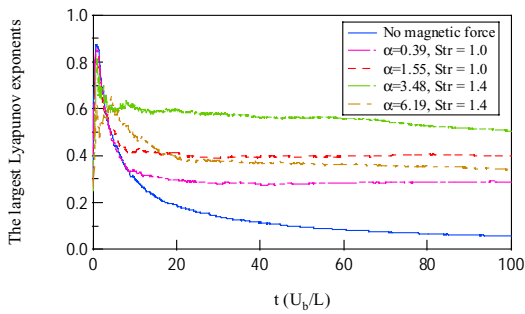


Fig. 6. Time traces of largest Lyapunov exponent under different forcing condition

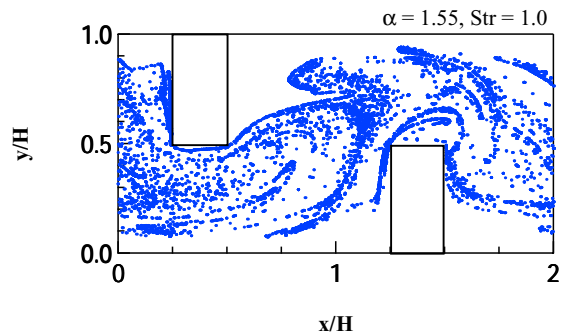


Fig. 7. Positions of beads with magnetic force ( $\alpha = 1.55, Str = 1.0$ ; ensemble in Phase I).

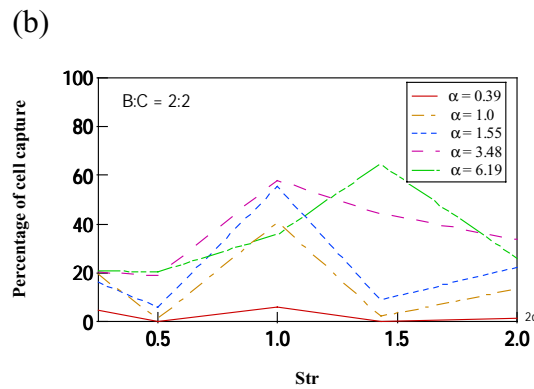
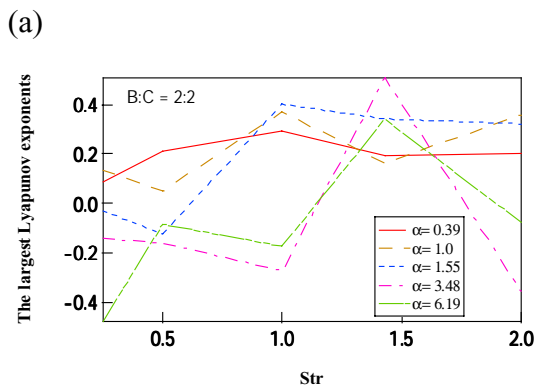


Fig. 7. Efficiency of mixing and cell capture in various conditions.

(a) Largest Lyapunov exponent,  $\lambda$ ; (b) Contact ratio,  $\gamma$ .

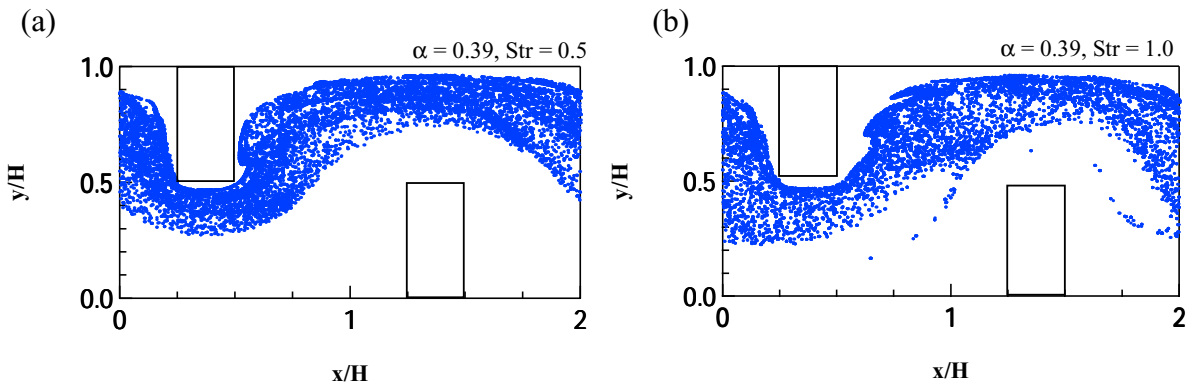


Fig. 8. Ensemble of beads positions in Phase I. (a)  $\alpha = 0.39$ ,  $Str = 0.5$ ; (b)  $\alpha = 0.39$ ,  $Str = 1.0$ .

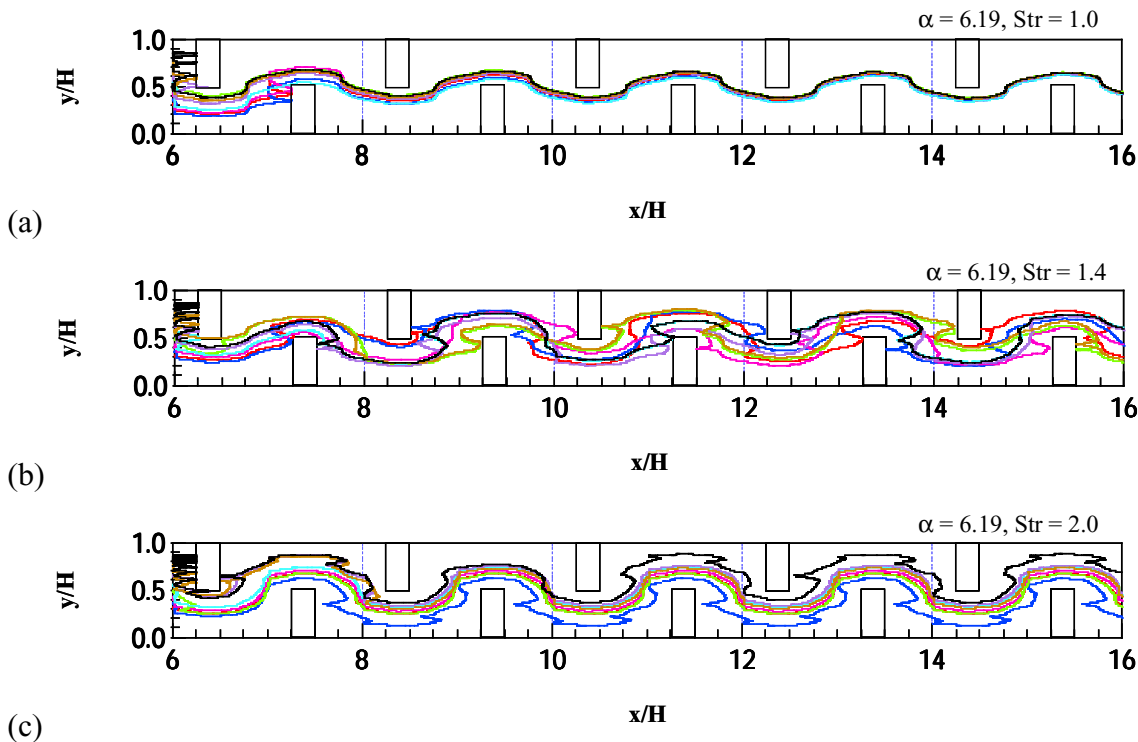


Fig. 9. Trajectories of beads at  $\alpha = 6.19$ . (a)  $Str = 1.0$ ; (b)  $Str = 1.4$ ; (c)  $Str = 2.0$ .

does not necessarily give higher  $\lambda$ , while larger  $\alpha$  gives higher. The maximum values of  $\gamma$  are obtained at  $Str = 1.0$ , except for the case of  $\alpha = 6.19$  which gives the maximum value at  $Str = 1.4$ . The global maximum of  $\lambda$  is found at  $\alpha = 3.48$  and  $Str = 1.4$ . Under some conditions, e.g.,  $\alpha = 0.39$ , the value of  $\gamma$  is low in spite of positive  $\lambda$ . In such cases, most of the beads are mixed only within the upper half, as shown in Fig. 8. This suggests that even if  $\lambda$  is positive, mixing between beads and cells is not necessarily good. Therefore,  $\gamma$  is considered a more suitable index for the evaluation of the mixers for cell sorting systems.

Figure 9 shows the trajectories of 8 beads, which are evenly introduced in the upper half of the channel, in the case of  $\alpha = 6.19$ . At  $Str = 1.4$ , motion of beads fluctuates into lower part, too, as shown in Fig. 9b. This penetration into the lower part (cell region) results in the large value of  $\gamma$ . At  $Str = 1.0$  and  $Str = 2.0$ , the trajectories of different beads are close to each other, as shown in Figs. 9a and 9c. This is caused by a synchronization of the convection and the magnetic actuation. The figures suggest that the time for beads to be convected the half-length of one unit matches the duration time of two or more actuation phases. The beads are trapped around the conductors and released at the same timing. Thus, their trajectories are similar. Under these conditions, one cell is attached by many beads and it results in low values of  $\gamma$ .

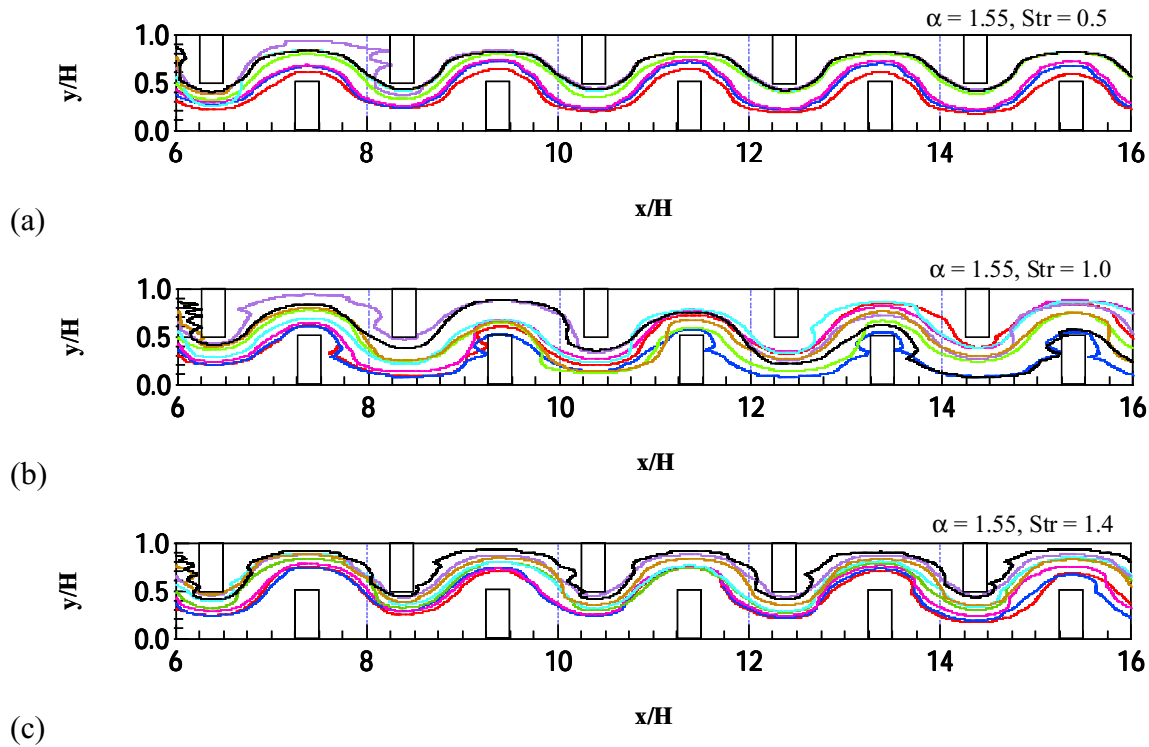


Fig. 10. Trajectories of beads at  $\alpha = 1.55$ : (a)  $Str = 0.5$ ; (b)  $Str = 1.0$ ; (c)  $Str = 1.4$ .

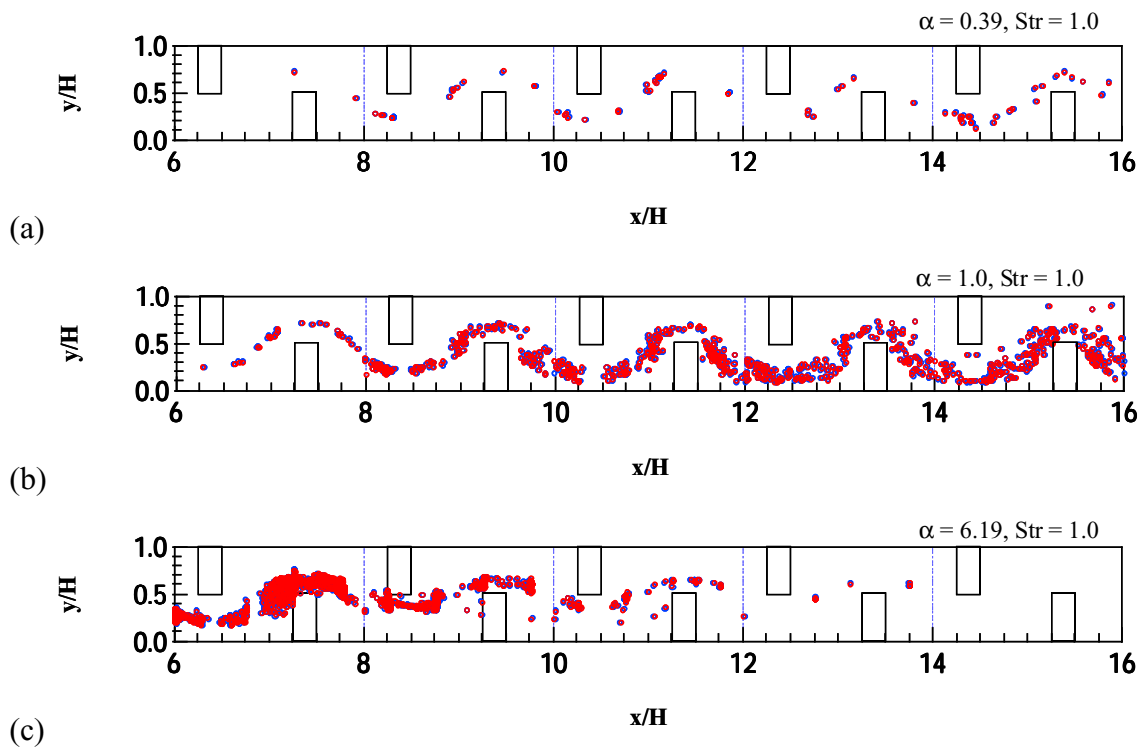


Fig. 11. Positions of first contact.

(a)  $\alpha = 0.39, Str = 1.0$ ; (b)  $\alpha = 1.0, Str = 1.0$ ; (c)  $\alpha = 6.19, Str = 1.0$ .

The mechanism to yield large values of  $\gamma$  is different for  $\alpha \leq 1.55$ , as shown in Fig. 10. Trapping of beads around the conductors is not observed. At  $Str = 1.0$ , the trajectories have mean drifts (or wave components much longer than the length of one unit), by which the beads deeply penetrate into the cell region.

Figure 11 shows the positions where the beads attach the cells at the first time. At  $\alpha = 0.39$ , a few beads attach onto cells. Contacts occur only in the area near the interface between bead and cell regions, because the magnetic force is too weak to move the beads further into the cell regions. At  $\alpha = 1$ , the number of contacts gradually increases in the downstream units. Most of the contact positions are in the lower part of mixer (cell region). This is caused by the drifting as mentioned above. For larger  $\alpha$ , many of the contact positions are found in the upstream mixer units. The contact positions are mostly found in the bead-trapping regions explained above.

In the analyses above, the number ratio of beads to cells is fixed to be unity. Here, we investigate on the effects of number ratio. The number of beads is 1.5 times and that of cells is 0.5 times as many as the original. The original and new cases denoted, respectively, as B:C = 2:2 and B:C = 3:1. The value of  $\gamma$  is higher with B:C = 3:1. Dependency of  $\gamma$  on  $\alpha$  and  $Str$  is similar to that in the case of B:C = 2:2. This similarity of dependency is more clearly illustrated in Fig. 12, which shows the correlation between  $\gamma$  with B:C = 3:1 and that with B:C = 2:2 (plotted for all the combination of  $\alpha$  and  $Str$ ). With B:C = 3:1, the contact ratio is increased by 48 % as compared to the case of B:C = 2:2.

Finally, the relation between the normalized cost function,  $J/\ell$ , and the contact ratio,  $\gamma$ , is shown in Fig. 13 for these two cases of B:C. This suggest that, for the present case, the number ratio of unity is better in terms of the operation cost, although the contact ratio can be increased by using larger number of beads.

#### 4. Conclusions

We have numerically investigated the enhancement of mixing of beads and cells for cell sorting by introducing a time-varying magnetic force in a micro serpentine conduit. The magnetic force conditions are in the range of  $0.25 \leq Str \leq 2.0$  and  $0.39 \leq \alpha \leq 6.19$ . From the simulation results, we have reached the following conclusions:

- (1) In order to measure the efficiency of mixing of beads and cells, the number of cells attached by immuno-magnetic beads (contact number) or its ratio (contact ratio) to the total number of cells is a more suitable measure than the conventionally used largest Lyapunov exponent.
- (2) Whether the beads access into the cell region depends on the relative velocity of beads

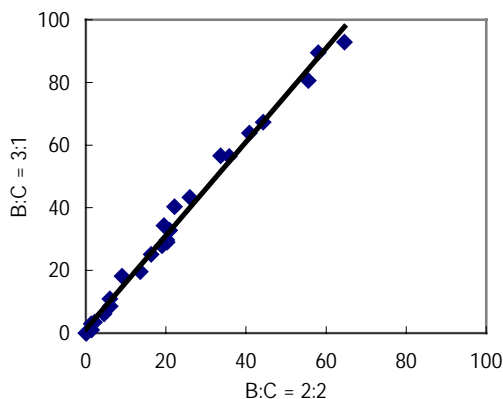


Fig. 12 Correlation between contact ratios for the cases of B:C=3:1 and B:C=2:2.

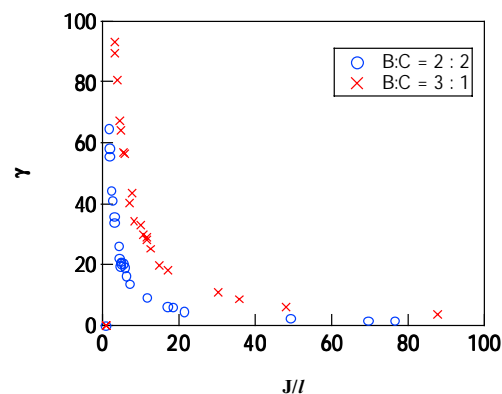


Fig. 13. Contact ratio versus normalized cost function for different number ratios (B:C).

increased by the magnetic force, i.e.,  $\alpha = u_R/U_b$ . The number of cells captured by beads increases as the increase of  $\alpha$ .

- (3) The Strouhal number of the magnetic actuation,  $Str$ , directly affects the dispersion of beads. A larger amount of dispersion (thus, a higher contact ratio) is attained when  $Str = 1.0$  except for the case with very large magnetic force, where the magnetic beads are trapped near the conductors.
- (4) At the same number density of particles, number ratio of beads to cells yields a higher percentage of cell capture. In terms of the cost of beads, however, the efficiency is better when the number ratio of beads to cells is unity.

## Acknowledgments

The authors are grateful to Dr. H. Suzuki (IIS, The Univ. of Tokyo) for valuable comments given at the initial stage of this work. This work was supported through the Grant-in-Aid for Scientific Research (S) by the Ministry of Education, Culture, Sports, Science and Technology of Japan (MEXT). Participation to conference of the first author was also supported by MEXT through The Univ. of Tokyo 21st Century COE Program "Mechanical Systems Innovation."

## References

1. Branebjerg, J., Gravesen, P., Krog, J.P., and Nielsen, C.R., 1996. Fast mixing by lamination. In: Proc. Annu. Workshop on MEMS, 441-446.
2. Beebe, D.J., Adrian, R.J., Olsen, M.G., Stremmer, M.A., Aref, H., and Jo, B.H., 2001. Passive mixing in microchannels: fabrication and flow experiments. *Med. Ind.*, 2, 343-348.
3. Chalmers, J.J., Zborowski, M., Sun, L., and Moore, L., 1998. Flow through, immunomagnetic cell separation. *Biotechnol. Prog.*, 14, 141-148.
4. Deval, J., Tabeling, P., and Ho, C.H., 2002. A dielectrophoretic chaotic mixer. In: Proc. IEEE Int. Conf. MEMS '02, 36-39.
5. Ho, C.H., and Tai, Y.C., 1998. Micro-Electro-Mechanical-Systems (MEMS) and fluid flows. *Annu. Rev. Fluid Mech.*, 30, 579-612.
6. Niu, X. and Lee, Y.K., 2003. Efficient spatial-temporal chaotic mixing in microchannels. *J. Micromech. Microeng.* 13, 454-462.
7. Ottino, J.M. 1989. *The Kinematics of Mixing: stretching, Chaos, and Transport*, New York, Cambridge University Press.
8. Suzuki, H., Ho, C.-M., and Kasagi, N., 2004. A chaotic mixer for magnetic bead-based micro cell sorter. *J. MEMS* (to appear).
9. Sprott, J. 2000. Numerical calculation of largest Lyapunov exponent. [http:// sprott. physics. wisc. edu / chaos/ lyapex.htm](http://sprott.physics.wisc.edu/chaos/lyapex.htm)
10. Volpert M., Meinhart C.D., Mezic I., and Dahel M., 2002. Modeling and numerical analysis of mixing in an actively controlled micromixer. In: Proc. 1st Int. Conf. on Heat Transfer, Fluid Mechanics, and Thermodynamics, Kruger Park, South Africa.